

Quark pair simulation near threshold : Reweighting and hadronization

M. Boonekamp ¹

CE-Saclay, F-91191 Gif-sur-Yvette Cedex, France

Abstract

Methods are presented allowing a realistic, experiment-based simulation of low-mass quark pairs coupling to a virtual photon. Differential cross-section reweighting factors allow to reproduce the resonant structure observed near quark pair production thresholds, and an algorithm is proposed that allows hadronization of the light quarks in the very low mass region, where existing theory-based models are expected to break down. The corresponding routines can be embedded in two- and four-fermion generators for e^+e^- machines.

1 Introduction

Several physics subjects of interest require a correct description of low mass quark-antiquark systems. In $e^+e^- \rightarrow q\bar{q}$ processes, initial state radiation can bring back the mass of the outgoing quark pair near its production threshold, giving rise to topologies with an energetic photon and a collimated hadronic system. Such events can for example be used to extract a measurement of the hadronic cross-section at the effective center-of-mass energy (and the ratio R of hadronic to pointlike muonic cross-sections) [1], or represent a background to searches for physics beyond the standard model, such as radiative decays of intermediate vector bosons.

In neutral-current $e^+e^- \rightarrow q\bar{q}f\bar{f}$ processes, low-mass quark pairs give again access to hadronized virtual photons. Such events are interesting in their own right (they have been studied by the LEP experiments at LEP1 [2], and the corresponding cross-section is measured by the Delphi experiment at LEP2 [3]), but can also represent a background to new particle searches, of which low mass Higgs boson searches are an example.

Current two- and four-fermion generators are not adapted to these kinds of studies. A first point is that the string model [4], upon which the PYTHIA program [5] relies to simulate the hadronization of parton systems, describes the data well at high energy, but is expected

¹ e-mail address: Maarten.Boonekamp@cern.ch

to break down below about 2 GeV. Secondly, computations of amplitudes generally make use of state-of-the-art knowledge of electroweak corrections and include a first order QCD term, but ignore non-perturbative corrections to vertices involving a light $q\bar{q}$ pair. In other words, diquark systems are generated with distorted mass distributions in the low mass region, and are hadronized unrealistically.

Low mass quark-antiquark pairs appearing in e^+e^- annihilations most often involve a coupling to a virtual photon. This suggests using experimental data on $e^+e^- \rightarrow$ hadrons a low energy, namely the R-ratio and measurements of exclusive final states cross-sections, to solve the problem. The mass spectrum and hadronization aspects are described in turn in the next two sections. Although it is not the main subject of this report, some results for two- and four-fermion processes are summarized in the third section. The code location is given in the last section.

2 Quark-pair production near thresholds

The task of implementing non-perturbative QCD corrections to $q\bar{q}$ differential cross-sections was first attempted in the framework of the four-fermion generator FERMISV [6,7]. The present method is similar and improves on a few shortcomings : the integration of the $q\bar{q}$ spectra are improved using proper Monte-Carlo techniques ; most importantly, recent data in the charm resonance region are used in order to obtain a good description of this mass range.

2.1 Reweighting of the $\gamma^*q\bar{q}$ vertex

With QCD turned off, the cross-section for quark pair production through a virtual photon can be written (in a symbolic way):

$$\begin{aligned} d\sigma_{hadrons}^0 &= d\sigma_{u\bar{u}}^0 + d\sigma_{d\bar{d}}^0 + d\sigma_{s\bar{s}}^0 + d\sigma_{c\bar{c}}^0 + d\sigma_{b\bar{b}}^0 \\ &= d\sigma_{\mu\mu} \times (R_u^0 + R_d^0 + R_s^0 + R_c^0 + R_b^0) \\ &= d\sigma_{\mu\mu} \times R^0, \end{aligned}$$

where the R_q^0 are just charge, colour and threshold factors, already taken into account in generators, and R^0 is the total parton level R-ratio. We now consider QCD effects, and write similarly:

$$\begin{aligned} d\sigma_{hadrons} &= d\sigma_{\mu\mu} \times R \\ &= d\sigma_{\mu\mu} \times (R_u + R_d + R_s + R_c + R_b) \\ &= d\sigma_{u\bar{u}}^0 \bar{R}_u + d\sigma_{d\bar{d}}^0 \bar{R}_d + d\sigma_{s\bar{s}}^0 \bar{R}_s + d\sigma_{c\bar{c}}^0 \bar{R}_c + d\sigma_{b\bar{b}}^0 \bar{R}_b, \end{aligned}$$

with $\bar{R}_q \equiv R_q/R_q^0$. The above lines express that for a given quark flavour q, a QCD-

improved description can be implemented by multiplying the parton level matrix elements by a factor \bar{R}_q , representing the contribution of quark flavour q to the experimental R-ratio, with charge, colour and threshold factors divided out ². Cross-sections of processes containing a $q\bar{q}$ pair will thus be computed as

$$d\sigma = \bar{R}_q(m_{q\bar{q}}) \times |\mathcal{M}|^2 \times dPh,$$

with $|\mathcal{M}|^2$ the parton level matrix elements, and \bar{R}_q evaluated at the $q\bar{q}$ mass.

The parametrization of R includes the contributions from all $J^{PC} = 1^{--}$ resonances up to the $\Upsilon(11020)$, with parameters taken from [8]. Intuitively (and as in [7]), the ρ 's and ω 's are attributed to the u- and d-quarks (*ie*, entered in the definitions of \bar{R}_u and \bar{R}_d); the ϕ 's, the ψ 's and the Υ 's are attributed to s-, c- and b-quarks (included in $\bar{R}_s, \bar{R}_c, \bar{R}_b$) respectively.

The continuum is parametrized by simple functions satisfying partonic boundary conditions, with parameters adjusted in the threshold regions so that the available data [9] are correctly reproduced. At present, one such function is defined for u- and d-quarks, one for s-quarks, and one for c-quarks. Since the currently available data do not allow a detailed representation of the Upsilon resonance region, the continuum from b-quarks is represented by a step function at the B-meson threshold.

Finally, the continuum parametrizations include an overall second order perturbative QCD correction factor. The running of the strong coupling constant is computed at second order, and Λ_{QCD} is set so as to reproduce the world-averaged $\alpha_S(m_Z^2)$ [8]. The implementation used is taken from [5].

The resulting parametrization of the R-ratio is illustrated in Figure 1.

2.2 Monte-Carlo sampling

The R function being very accidented, special attention has to be paid to its Monte-Carlo sampling. Exploration of all narrow peaks is performed using iterative dividing of the integration range. In a first step, the full range is divided in a number of sub-intervals, the borders of which are set on the (a priori known) peaks of the resonances. The interval contributing most to the integral is then divided into two equal sub-intervals. This process is iterated and fine granularity is obtained by requiring a large number of intervals. After completion of the initialization phase, drawing intervals at random (in proportion to their contribution to the total integral) then ensures correct population of all the peaks. The program implementing this algorithm and used for our purpose, **VESKO**, was first described in [10]. It was modified to be able to take into account the positions of a priori known peaks in the distributions, and to handle several distributions simultaneously.

² Of course, the splitting of R into contributions from different flavours is only a computational convenience, and the whole procedure makes sense only after summing all contributions.

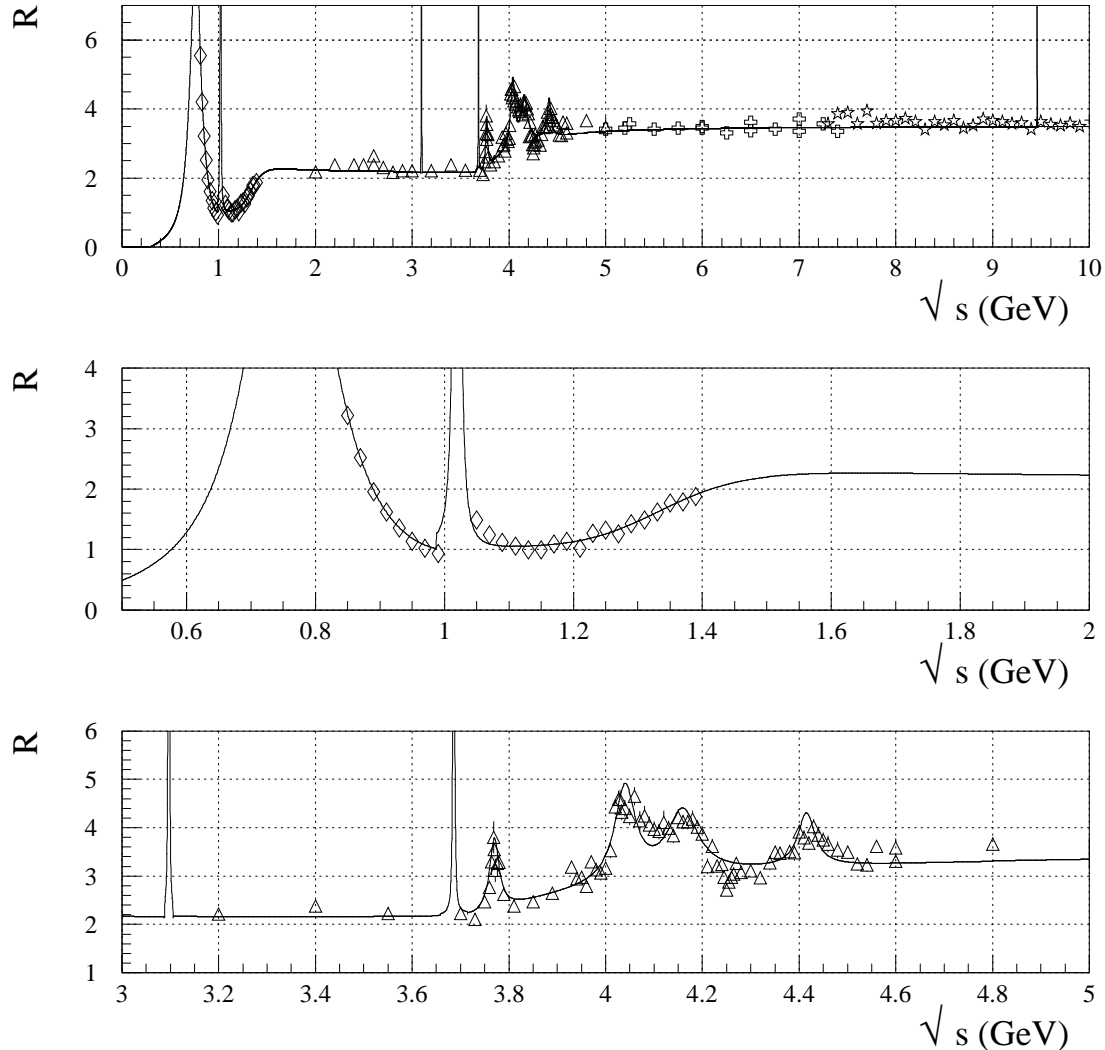


Fig. 1. Parametrization of the R-ratio, and comparison to various data sets. The upper figure illustrates the range between 0 and 10 GeV. The data sets are from ND (below 1.5 GeV), BES (from 2 to 5 GeV), Crystal Ball (from 5 to 7.4 GeV) and MD-1 (between 7.4 and 10 GeV) [9]. The middle figure details the ϕ region, and the lower one shows the Ψ resonance region.

2.3 Caveats

The above procedure is valid only if the final state quark pair is genuinely coupled to a virtual photon. Therefore, this method should not be applied to the $e^+e^- \rightarrow e^+e^-q\bar{q}$ process, unless a kinematic region is selected where the multi-peripheral (mostly $\gamma\text{-}\gamma$) diagrams have negligible contribution and interference with the other diagrams.

Other complications appear for final states with four quarks. In principle, one \bar{R} factor should be present for every pair of identical quarks, but there are cases where care should be taken. For example, in the $u\bar{d}\bar{d}u$ final state and if all quarks have same colour,

one should evaluate whether charged current diagrams (*ie*, WW production) or neutral current diagrams (Z/γ^* Z/γ^*) dominate the total amplitude, depending on momentum configurations. Similarly, in final states with four identical quarks (of same colour), the “pairing” which dominates the total amplitude has to be determined, and the \bar{R} factors should be evaluated at the masses of the connected quark pairs.

On the contrary, the $e^+e^- \rightarrow q\bar{q}$ process is unambiguous.

3 Hadronization

Having decided on the $q\bar{q}$ mass spectrum in the resonance region, it remains to be determined how every individual event should behave in the detector. As a function of the mass of the quark pair, it has to be decided whether we it can be treated as a resonance of known decay properties, and if not, if the string or cluster fragmentation algorithms available in PYTHIA will work. In the first case, the quark pair is replaced by the corresponding resonance in the PYTHIA event record, and it is decayed by a subsequent call to the hadronization routine. In the second case, it is assumed that above a mass of 2 GeV, string hadronization is convenient, except in the $c\bar{c}$ and $b\bar{b}$ threshold regions where cluster hadronization correctly takes over.

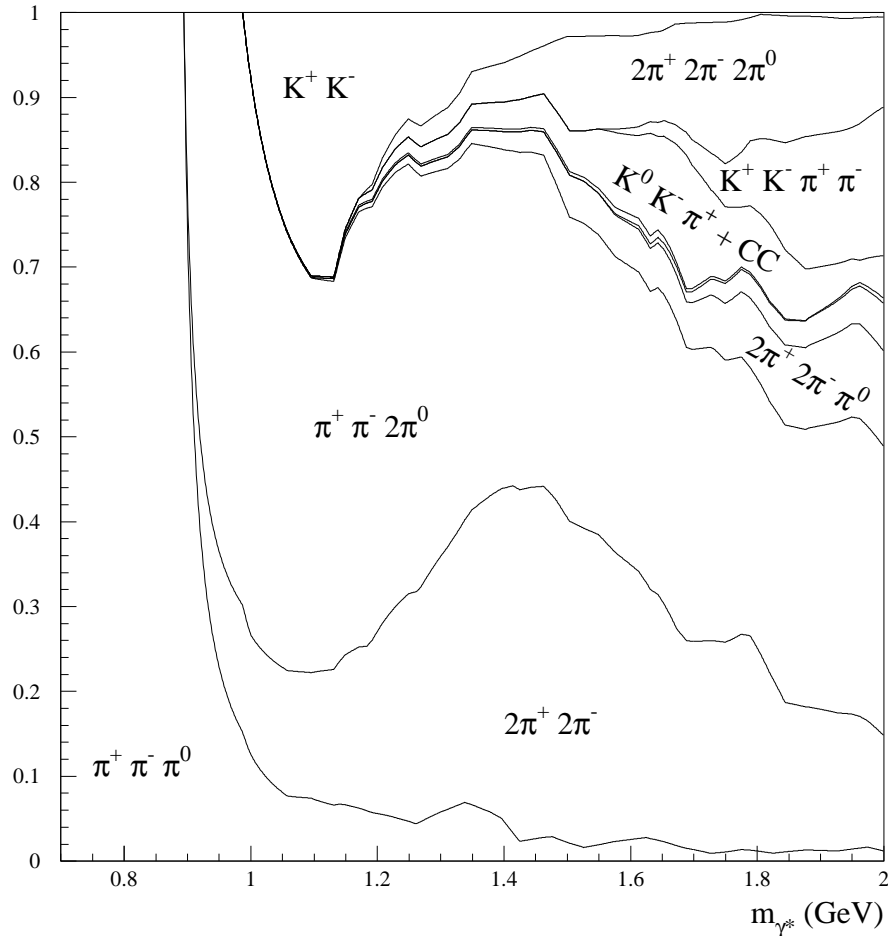
Since the lowest mass region is dominated by the ρ , we are left with a mass window between ~ 0.9 and 2 GeV, open to u-, d-, and s-quarks, where new input is needed. This input can be taken from experiment, since the first hadronic final states in e^+e^- collisions have been extensively studied in the seventies and eighties. Data on the following exclusive non-resonant cross-sections [11] were compiled for this purpose:

- $e^+e^- \rightarrow 3\pi$ ($\pi^+\pi^-\pi^0$),
- $e^+e^- \rightarrow 4\pi$ ($2\pi^+2\pi^-, \pi^+\pi^-2\pi^0$),
- $e^+e^- \rightarrow 5\pi$ ($2\pi^+2\pi^-\pi^0$),
- $e^+e^- \rightarrow 6\pi$ ($2\pi^+2\pi^-2\pi^0, 3\pi^+3\pi^-$),
- $e^+e^- \rightarrow 2K$ ($K^+K^-, K_S K_L$),
- $e^+e^- \rightarrow K_S K^+ \pi^- + CC$,
- $e^+e^- \rightarrow K^+ K^- \pi^+ \pi^-$.

The $K_L K^+ \pi^-$ final state has never been measured due to experimental difficulties related to K_L detection, but was assumed to be equal to the $K_S K^+ \pi^-$ cross-section.

These cross-sections define the “branching fractions” of the non-resonant γ^* , which are displayed in figure 2. In practice, when a $q\bar{q}$ pair is found to be neither a resonance, nor heavy enough to be administrated by string fragmentation, one of the above final states is drawn at random according to the measured cross-sections at the current $q\bar{q}$ mass. The momenta of the outgoing hadrons are then generated uniformly in the available phase space using the CERN routine GENBOD [12] (it has currently not been attempted to reproduce the inner kinematic structure of these multiparticle final states. For example, it is ignored that a significant part of the $2\pi^+2\pi^-$ final state is genuinely $\rho\rho$ decays). Finally, the quark pair is replaced by its daughter hadrons in the PYTHIA event record.

Fig. 2. The non-resonant (ρ and ϕ subtracted) branching fractions of the γ^* as a function of its mass, from measurements of $e^+e^- \rightarrow$ exclusive final states [11].



4 Results for specific processes

The present algorithm has been implemented in the 2-fermion generator KK2f [13]. Running this generator in the configuration of current e^+e^- colliders allows to estimate the radiative hadronic cross-sections expected at these machines. Table 1 summarizes results for the existing Φ - and B-factories, and for a hypothetical Charm factory such as the Cleo-c program at CESR. Given the expected luminosities at these machines, $\mathcal{O}(10^6 - 10^7)$ events are expected in regions where the knowledge of the hadronic cross-section is still limited³. Figure 3 illustrates the differential hadronic cross-sections expected when operating at D- and B-meson threshold.

In the context of four-fermion processes, events with a light quark-pair will show up as thin, collimated jet (most often a $\pi^+\pi^-$ pair from a ρ decay) recoiling against an energetic lepton- or jet-pair. Table 2 summarizes some results for the $\mu^+\mu^-q\bar{q}$ and $q\bar{q}q\bar{q}$ processes. Assuming 500 fb^{-1} recorded per experiment, the number of expected events with one

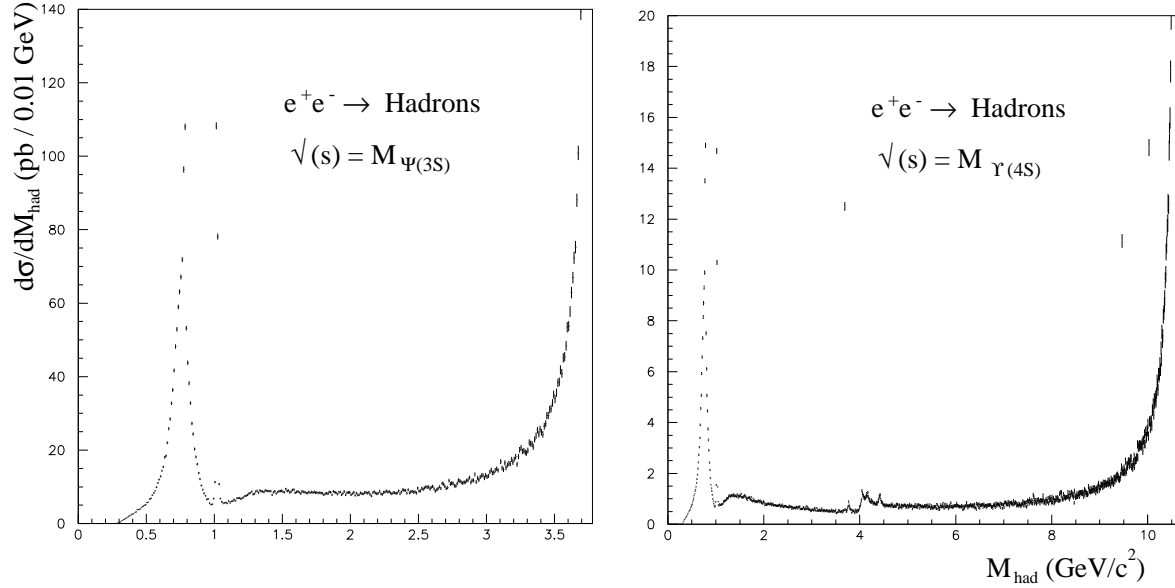
³ These numbers are given with initial state radiation computed to third order (see [13]), and final state radiation switched off. A discussion on the level of accuracy of this approximation is beyond the scope of this work, but is expected to be 1-2%.

Table 1

Expected $e^+e^- \rightarrow q\bar{q}$ event rates (in nanobarn) for various colliders. Cross-sections are given for three ranges of the effective center-of-mass energy (for the hypothetical Charm factory operating on the $\Psi(3S)$, the last number corresponds to the range 2-3 GeV). No selections are applied.

Collider	\sqrt{s} (GeV)	0-0.95 GeV	1.05-2 GeV	2-5 GeV
DAΦNE	1.02	42.38		
Charm factory	3.77	1.31	0.77	0.95*
KEKB,PEP-II	10.58	0.18	0.09	0.25

Fig. 3. Differential radiative cross-sections expected at the $\Psi(3S)$ resonance (left) and at the $\Upsilon(4S)$ resonance (right). No selections are applied.



quark pair of mass smaller than 2 GeV is $\mathcal{O}(10^1 - 10^2)$, depending on the process under consideration. This confirms that such events can represent a substantial background to new particle searches, and need to be accounted for in the simulation of standard model processes.

Table 2

Expected $e^+e^- \rightarrow \mu^+\mu^-q\bar{q}$ and $q\bar{q}q\bar{q}$ event rates (in picobarn) at LEP2 energies. Quark-pair masses are restricted above 2 GeV (case 1), and released down to threshold (case 2).

Final state	\sqrt{s} (GeV)	Case 1	Case 2
$\mu^+\mu^-q\bar{q}$	200	0.33	0.36
$q\bar{q}q\bar{q}$	200	8.72	9.05

5 Program availability

The routines implementing the methods described above are obtainable from [14], together with installation notes and commented example applications.

6 Conclusions

A complete treatment of low-mass quark pair production and hadronization is described, which is relevant whenever the pair is produced via a virtual photon. This allows to release traditional cuts on quark pair invariant masses, and to study low mass hadronic systems specifically. The large statistics available at existing e^+e^- machines will allow to compare these predictions with experiment, with applications both in two- and four-fermion processes.

References

- [1] See, for example:
S. Binner, J. H. Kühn, K. Melnikov, Phys. Lett **B459** (1999) 279;
K. Melnikov, F. Nguyen, B. Valeriani, G. Venanzoni, Phys. Lett. **B477** (2000) 114;
S. Spagnolo, Eur. Phys. J. **C6** (1999) 637.
- [2] ALEPH Collaboration, Z. Phys. **C66** (1995) 3;
DELPHI Collaboration, Nucl. Phys. **B403** (1993) 3;
L3 Collaboration, Phys. Lett. **B321** (1994) 283;
OPAL Collaboration, Phys. Lett **B287** (1992) 289.
- [3] DELPHI Collaboration, *Measurement of the four-fermion final states mediated by neutral current processes*, Contribution to HEP'01 and Lepton-Photon'01, DELPHI 2001-096 CONF 524
- [4] B. Andersson, G. Gustafson, G. Ingelman, T. Sjöstrand, Phys. Rep. **97** (1983) 31 ;
T. Sjöstrand, Nucl. Phys. **248** (1984) 469.
- [5] T. Sjöstrand, Comput. Phys. Commun. **82** (1994) 74.
- [6] J. Hilgart, R. Kleiss, F. Le Diberder, Comput. Phys. Commun. **75** (1993) 191.
- [7] ALEPH Collaboration, Z. Phys. **C66** (1995) 3.
The modified version of FERMISV can be found at:
<http://alephwww.cern.ch/~janot/Generators.html>.
- [8] Particle Data Group, Eur. Phys. J. **C15** (2000) 1.
- [9] ND Collaboration, Phys. Rep. **202** (1991) 99;
BES Collaboration, Phys. Rev. Lett. **84** (2000) 594;
BES Collaboration, hep-ex/0102003;
C. Edwards et al, SLAC-PUB-5160;
MD-1 Collaboration, Phys. Rep. **267** (1996) 71.

- [10] S. Jadach, W. Placzek,
Comput. Phys. Commun. **72** (1992) 221.
- [11] ADONE Collaboration, Nucl. Phys. **B31** (1981) 445;
DM1 Collaboration, Phys. Lett. **B99** (1981) 261;
DM1 Collaboration, Phys. Lett. **B107** (1981) 145;
DM1 Collaboration, Phys. Lett. **B110** (1982) 335;
DM1 Collaboration, Phys. Lett. **B112** (1982) 178;
OLYA Collaboration, Phys. Lett. **B107** (1981) 297;
DM2 Collaboration, Zeit. Phys. **C39** (1988) 13;
ND Collaboration, Phys. Rep. **202** (1991) 99;
DM2 Collaboration, Zeit. Phys. **C56** (1992) 15.
- [12] F. James, Monte-Carlo Phase Space, CERN 68-15 (1968).
- [13] S. Jadach, B.F.L. Ward, Z. Was, Comput. Phys. Commun. **130** (2000) 260.
The latest version, including this work, can be obtained at:
<http://jadach.home.cern.ch/jadach/KKindex.html>.
- [14] <http://boonekam.home.cern.ch/boonekam/hadgen.htm>